A Morphology-Based Spatial Consistency Algorithm to Improve EGM Delineation in Ventricular Electroanatomical Mapping

Alejandro Alcaine[1,2], David Soto-Iglesias[3], David Andreu[4], Juan Acosta[4], Antonio Berruezo[4], Pablo Laguna[1,2], Oscar Camara[3], Juan Pablo Martínez[1,2]

[1]Biomedical Signal Interpretation and Computational Simulation (BSICoS) Group, Aragón Institute of Engineering Research (I3A), IIS Aragón, Universidad de Zaragoza, Zaragoza, Spain.
[2]CIBER in Bioengineering, Biomaterials and Nanomedicine (CIBER-BBN), Madrid, Spain.
[3]PhySense Group, Universitat Pompeu Fabra, Barcelona, Spain.
[4]Arrhythmia Section, Cardiology Department, Thorax Institute, Hospital Clínic, Barcelona, Spain.

Abstract

Activation mapping using electroanatomical mapping (EAM) systems helps to guide catheter ablation treatment of common arrhythmias. In focal tachycardias, the earliest activation area becomes the ablation target. Recently, we proposed a single-point wavelet-based algorithm to automatically identify electrogram (EGM) activation onsets for activation mapping. In this work, we propose an EGM morphology-based spatially-consistent algorithm for improving activation mapping in areas with a high-density of mapping points. The algorithm aligns those EGMs spatially close and morphologically similar and checks if the detected bipolar EGM activation onset is determined within a tolerance of $\pm$ 5 ms. If not, a weighted average bipolar EGM activation signal is computed and delineated. Then, the new activation onset is used to compute the local activation time (LAT). Automatically detected onsets are compared with manual annotations obtained during ablation procedure by an expert technician in a total of 15 electroanatomical maps (1763 mapping points). The presented algorithm modifies 31% of the studied mapping points and in those cases reduces the difference with manual annotations from 5.1 $\pm$ 13 ms to 4.3 $\pm$ 11.6 ms.

1. Introduction

Ventricular tachycardia (VT) is often related with structural heart disease. However, about 10% of VT patients have no structural heart disease, and hence are known as idiopathic VT [1]. The most common origin of idiopathic VT arise from the outflow tract (OT) with a predominance from the right OT [2], but left OT is also frequent [3, 4].

Idiopathic ventricular outflow tract (IVOT) tachycardia has focal origin, therefore, identification of the earliest activation area becomes in the ablation treatment target. Activation mapping using an electroanatomical mapping (EAM) system helps to identify the earliest activation area [5]. The local activation time (LAT) is defined as the time instant when the catheter electrodes sense an activation wavefront with respect to a stable time point, typically used for activation mapping [1]. However there are different LAT definitions depending on the electrogram (EGM) signal acquisition mode [6].

Recently, a wavelet-based delineator has been proposed to automatically compute LATs based on the bipolar EGM activation onset [7]. It determines the bipolar EGM activation onset from the wavelet decomposition of the EGM activation signal envelope using the estimated QRS complex width as searching window. However, this single-point delineation strategy does not take profit of the spatial relations of the acquired mapping points which is of special interest in the definition of the ablation target area in IVOT tachycardias catheter ablation treatment.

Therefore, we proposed an EGM morphology-based algorithm that exploits the morphological similarities of spatially close mapping points in order to obtain smooth activation patterns. This is of especial interest when mapping IVOT tachycardias and there are high-density mapping points in the earliest activation area.

2. Materials

Clinical data used in this study consist of 15 electroanatomical maps (7 right ventricle and 8 left ventricle maps) of patients suffering from non-tolerated premature ventricular contraction (PVC) beats due to diagnosed IVOT tachycardia and referred to the arrhythmia section of Hospital Clínic de Barcelona (Barcelona, Spain) for catheter ablation procedure.

Each map was acquired using the CARTO® 3 system (*Biosense-Webster Inc., Diamond Bar, CA, USA*). The to-

tal number of studied mapping points was 1763 (118 ± 74 points per map). Each point includes standard 12-lead ECG signals and bipolar EGM signals from a NaviStar Thermocool® irrigated tip catheter (*Biosense Webster Inc., Diamond Bar, CA, USA*) 16-500 Hz band-pass filtered with a 50 Hz notch filter. Those signals were acquired at 1 kHz sampling frequency during 2.5 seconds, assuring that the contact of the catheter tip with the endocardial wall was stable and at least one PVC beat occurs during mapping.

For each mapping point, the activation onset of the distal bipolar EGM signal was determined manually, during the intervention, by an expert technician and were used for LAT measurement during activation mapping. Therefore, these manual annotations will be used in this study for performance evaluation.

3. Methods

The algorithm is applied after delineation of the EGM at each i-th mapping point, $x_i[n]$, using the wavelet-based method described in [7]. Each mapping point has associated the position vector $\boldsymbol{r}_i = [r_{x_i}, r_{y_i}, r_{z_i}]^\top$, given by the EAM system.

First, the algorithm searches across the already processed mapping points, $x_k[n], k = 1...i$, which are located in a neighbourhood N_i. This neighbourhood is defined as $N_i = \{k\ ;\ \|\boldsymbol{r}_i - \boldsymbol{r}_k\|_2 \leq 6\ \text{mm}\}$. Hence, those $x_k[n]$ which belong to N_i were selected as neighbour cluster candidates.

Next, an EGM morphology-based constraint is applied on these neighbour cluster candidate points ($k \in N_i$). This evaluation was made by means of the cross-covariance function:

$$C_{i,k}[m] = \sum_{n=-L/2}^{L/2} (x_i[n] - \bar{x}_i)(x_k[n+m] - \bar{x}_k), \quad (1)$$

where L is the window length spanning ±70 ms from de estimated QRS onset and end points, $\bar{x}_i$ and $\bar{x}_k$ are the mean values of $x_i[n]$ and $x_k[n]$, respectively, and m stand for the lag between signals. The cross-covariance delay between signals, $\tau_{i,k}$, is obtained as:

$$\tau_{i,k} = \arg\max_m \{C_{i,k}[m]\}. \quad (2)$$

Then, the cluster of neighbour and morphology similar points is defined as $S_i = \{k \in N_i\ ;\ C_{i,k}^{max} \geq 0.85\ \&\ \tau_{i,k} \leq \pm\ 10\ \text{ms}\}$.

All signals from the cluster points $x_k[n], k \in S_i$, were aligned with respect to $x_i[n]$ using the cross-covariance delay $\tau_{i,k}$ in order to check the LAT agreement between adjacent points. We consider that the current mapping point is consistently annotated if the difference between its identified LAT with the median LAT of the rest of the cluster points is below ± 5 ms. If this condition is not fulfilled, a weighted average EGM signal $x_{w,i}[n]$ is computed as follows:

$$x_{w,i}[n] = \frac{\sum_{k \in S_i} w_{i,k} \cdot x_k[n - \tau_{i,k}]}{\sum_{k \in S_i} w_{i,k}}, \quad (3)$$

where $w_{i,k}$ stands for the weights for each cluster signal $x_k[n]$, defined as:

$$w_{i,k} = \frac{C_{i,k}^{max} - 0.85}{1 - 0.85}, k \in S_i. \quad (4)$$

Finally, this weighted averaged EGM signal, $x_{w,i}[n]$, is delineated with the same wavelet-based delineator [7]. The resulting onset time, $n_{o,i}^w$, is associated to the current mapping point and a reliability value of the new mark is assigned as the median value of $C_{i,k}^{max}, k \neq i$.

For the rest of the clustered points in S_i, their single-point-computed LAT is modified to $n_{o,i}^w - \tau_{i,k}$, except if the same point had been previously assigned to another cluster with a greater maximum covariance than $C_{i,k}^{max}$.

Figure 1 shows a representative example of the presented algorithm on a fractionated EGM activation.

4. Results

The assessment of the presented algorithm was made by comparing the automatically obtained onsets (using or not the presented algorithm) with the activation onsets manually obtained by an expert technician during the intervention. Table 1 shows the difference of the automatic annotations with respect to the manual annotations. We study the performance of the presented algorithm in different subsets of points: 1) the whole database, 2) those points modified by the algorithm and 3) those points activated after the earliest activated point.

During ablation treatment of IVOT tachycardias, the objective of activation mapping is to identify the earliest activation area. We define as belonging to that area all those points activated within an interval of 10 ms after the earliest activated point. Hence, the third column of Table 1 shows the differences measured in those points. The presented algorithm provides less biased and more stable annotations of this area (3.9 ± 10.8 ms) than the single-point approach (4.3 ± 13.5 ms).

The second column of Table 1 shows the performance obtained in those points whose single-point activation onset is modified by the algorithm. A total of 31% mapping points were modified by the algorithm while the rest remain unchanged. In this subset, the differences are also shortened using the presented algorithm from 5.1 ± 13 ms to 4.3 ± 11.6 ms. Finally, all studied mapping points were

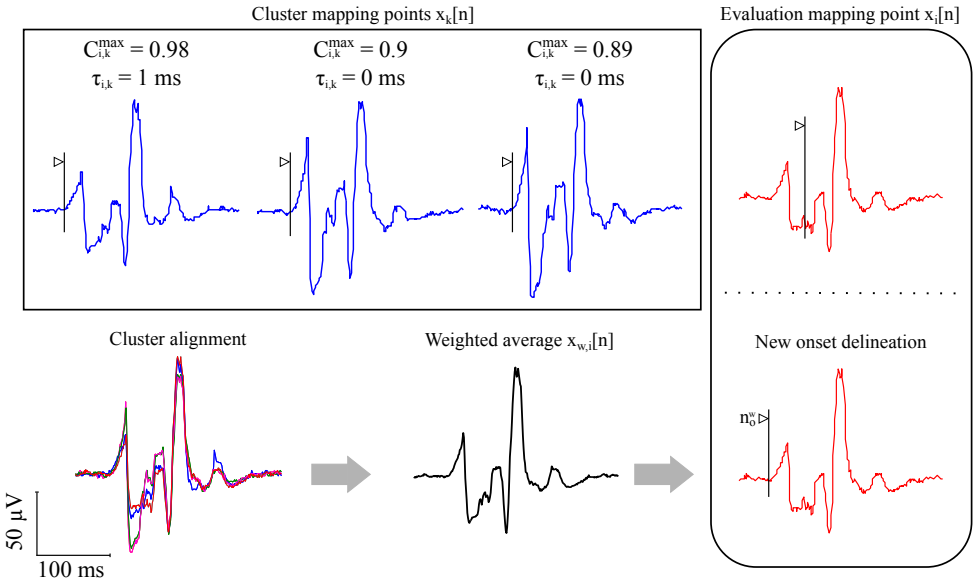

Figure 1. Example of activation onset modification of a fractionated EGM activation by the presented algorithm: Evaluation point $x_i[n]$ (red) is paired with three clustered mapping points $x_k[n]$ (blue). A weighted averaged EGM activation $x_{w,i}[n]$ is obtained (black) after alignment and annotation consistency checking. Finally, a new activation onset $n^w_{o,i}$ is identified and reassigned to $x_i[n]$. Activation onsets are indicated with black vertical lines pointed by a triangle.

considered in the first column of Table 1. It can be observed that using the proposed algorithm slightly improves the difference from 5 $\pm$ 13 ms to 4.8 $\pm$ 12.6 ms due to the dominance of the unchanged measurements. It is noteworthy that the difference bias is positive, hence, the automatic annotations identify slightly later LATs than the manual annotations.

Figure 2 shows a representative example of a reconstructed 3-D activation map (map #10) using the annotation sets of this work. Those 3-D maps are generated by discretizing the colorscale in 10 ms isochrone areas color-coded from red (earlier) to pink (later) and referenced to the QRS complex, as it is usually done in clinical practice [4]. The activation map obtained with the presented algorithm (Fig. 2(c)) shows a smoothed activation pattern than using the single-point approach (Fig. 2(b)). Moreover, the effective ablation site (red sphere pointed by white arrow) is close to the earliest activated area than using the single-point approach, but still not within it as shown the manual annotated map (Fig. 2(a)).

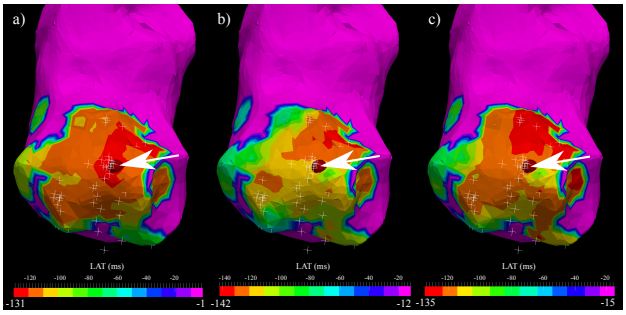

Figure 2. Example of activation maps obtained using: a) Manual annotations, b) automatic single-point annotations and c) automatic multi-point annotations. White crosses indicate the acquired mapping points and white arrow indicates the effective ablation site.

5. Discussion and conclusion

Activation mapping during catheter ablation treatments help to identify the earliest activation area in patients with IVOT tachycardia. Recently, a wavelet-based EGM onset identification algorithm was proposed for activation mapping [7]. However, this approach did not exploit spatial relation between mapping points. In this work, we propose a morphology-based spatially-consistent algorithm to improve activation mapping by exploiting such spatial relations, especially in the areas with high-density mapping.

Automatically obtained LATs (using and not using the proposed algorithm) were compared with those obtained during the ablation intervention by an expert technician. In the 10 ms earliest activation area, the proposed algorithm outperforms the single-point approach. This could be more beneficial if used in combination with high-density mapping catheters, which acquire multiple close EGMs with a single beat. Looking at the single map results, this im-

Table 1. Difference between manual and the automatic LATs (using or not the presented algorithm) for different sets of mapping points and for each studied map (mean ± SD). N/A: Not Applicable.

	All mapping points			Modified mapping points			10 ms earliest activated points		
Map (#)	Points (#)	Using [7] (ms)	This work (ms)	Points (#)	Using [7] (ms)	This work (ms)	Points (#)	Using [7] (ms)	This work (ms)
1	200	8.3 ± 10.1	8.5 ± 10.1	63	7.4 ± 9.3	7.9 ± 9	13	11 ± 8.3	12.2 ± 8.3
2	262	1 ± 8.7	1 ± 8.7	103	1.4 ± 7.5	1.4 ± 7.6	50	-0.8 ± 4.3	-0.8 ± 4.7
3	203	6.8 ± 11	6.8 ± 10.9	57	6.9 ± 9.1	6.8 ± 8.8	47	7.6 ± 10.4	7.7 ± 10.2
4	153	8.7 ± 13	9 ± 13.3	34	10.5 ± 11.9	11.8 ± 13.1	15	1.8 ± 9.6	1.8 ± 9.5
5	190	8.5 ± 13.3	8.3 ± 13.8	28	10 ± 17.6	8.5 ± 20.1	21	-3.1± 3.8	-3.1 ± 3.8
6	40	0.7 ± 17	0.9 ± 16.9	15	8.4 ± 12.3	8.9 ± 11.4	1	N/A	N/A
7	90	6.8 ± 11.6	6.3 ± 10.6	23	8.6 ± 16.8	6.7 ± 14.1	8	2.9 ± 9.2	3 ± 9.5
8	72	2.6 ± 9.7	1.8 ± 8	23	5.2 ± 12.4	2.6 ± 8.1	3	N/A	N/A
9	42	12.2 ± 13	12.4 ± 12.9	15	17.1 ± 10.4	17.7 ± 9.6	2	N/A	N/A
10	87	0.8 ± 21.2	-1.2 ± 14.6	28	3.4 ± 28,4	-2.7 ± 7.6	27	6.4 ± 26.6	1.7 ± 8.3
11	38	-0.4 ± 7.1	-0.2 ± 7.2	15	0.8 ± 6	1.3 ± 6.1	16	1.5 ± 4.5	1.6 ± 4.7
12	189	2.3 ± 10.1	2.4 ± 10.9	91	1 ± 8.8	0 ± 10.4	25	4.2 ± 6.8	4.4 ± 7
13	90	-5.2 ± 11.9	-5.7 ± 11.9	26	-4 ± 8.8	-5.9 ± 8.7	38	-2.6 ± 7.6	-2.2 ± 6.7
14	55	14.1 ± 19.9	13.8 ± 19.7	18	14.7 ± 15	13.8 ± 14.2	12	26.2 ± 12.3	26.1 ± 12.2
15	52	6.6 ± 14.4	5.2 ± 12.9	9	10.9 ± 19.1	3.1 ± 10.8	16	12.8 ± 19.8	9.7 ± 18.2
Total	1763	5 ± 13	4.8 ± 12.6	548	5.1 ± 13	4.3 ± 11.6	294	4.3 ± 13.5	3.9 ± 10.8

provement is slight or even nonexistent, however the improvement is remarkable in some maps with high differences using the single-point approach. It must also be noted that differences are computed with respect to manual annotations performed by a technician during the intervention, which have an intrinsic variability, and are not free of errors.

The results of this work show that the proposed method allows to obtain smoother activations maps that could potentially improve ablation treatments of IVOT tachycardias helping in the decision process of determining it origin (right OT vs. left OT) and the ablation target [4].

Acknowledgements

This study was supported by a F.P.I. grant to A.A. ref.: BES-2011-046644, by projects TEC2010-21703-C03-02, TEC2013-42140-R and TIN2011-28067 from MINECO. Also by Aragón Government (Spain) and ESF (EU) through Grupo Consolidado BSICoS ref.: T96. The CIBER-BBN is an initiative of Instituto de Salud Carlos III.

References

[1] Aliot EM, Stevenson WG, Almendral-Garrote JM, Bogun F, Calkins CH, Delacretaz E, Bella PD, Hindricks G, Jaïs P, Josephson ME, Kautzner J, Kay GN, Kuck KH, Lerman BB, Marchlinski F, Reddy V, Schalij MJ, Schilling R, Soejima K, Wilber D. EHRA/HRS expert consensus on catheter ablation of ventricular arrhythmias. Europace 2009;11(6):771–817.

[2] Movsowitz C, Schwartzman D, Callans DJ, Preminger M, Zado E, Gottlieb CD, Marchlinski FE. Idiopathic right ventricular outflow tract tachycardia: Narrowing the anatomic location for successful ablation. American heart journal 1996;131(5):930–936.

[3] Lerman BB, Stein KM, Markowitz SM. Mechanisms of idiopathic left ventricular tachycardia. Journal of Cardiovascular Electrophysiology 1997;8(5):571–583.

[4] Herczku C, Berruezo A, Andreu D, Fernández-Armenta J, Mont L, Borràs R, Arbelo E, Tolosana JM, Trucco E, Ríos J, Brugada J. Mapping data predictors of a left ventricular outflow tract origin of idiopathic ventricular tachycardia with V3 transition and septal earliest activation. Circulation Arrhythmia and Electrophysiology 2012;5(3):484–491.

[5] Issa Z, Miller JM, Zipes DP. Clinical Arrhythmology and Electrophysiology: A Companion to Braunwald's Heart Disease. 2 edition. Saunders, 2012.

[6] Paul T, Moak JP, Morris C, Garson Jr. A. Epicardial mapping: How to measure local activation?. Pacing and Clinical Electrophysiology 1990;13(3):285–292.

[7] Alcaine A, Soto-Iglesias D, Andreu D, Fernández-Armenta J, Berruezo A, Laguna P, Camara O, Martínez JP. A wavelet-based electrogram onset delineator for automatic ventricular activation mapping. IEEE Transactions on Biomedical Engineering 2014;DOI 10.1109/TBME.2014.2330847.

Address for correspondence:

Alejandro Alcaine Otín
C/ Mariano Esquillor S/N, Edificio I+D+i, L 4.0.05
50018 Zaragoza, Spain.
E-mail: aalcaineo@unizar.es